

# Identity Authentication in Two-Subject Environments Using Microwave Doppler Radar and Machine Learning Classifiers

Shekh M. M. Islam<sup>✉</sup>, *Member, IEEE*, Olga Borić-Lubecke, *Fellow, IEEE*, and Victor M. Lubecke<sup>✉</sup>, *Fellow, IEEE*

**Abstract**—Identity authentication based on Doppler radar respiration sensing is gaining attention as it requires neither contact nor line of sight and does not give rise to privacy concerns associated with video imaging. Prior research demonstrating the recognition of individuals has been limited to isolated single-subject scenarios. When two equidistant subjects are present, identification is more challenging due to the interference of respiration motion patterns in the reflected radar signal. In this research, respiratory signature separation techniques are functionally combined with machine learning (ML) classifiers for reliable subject identity authentication. An improved version of the dynamic segmentation algorithm (peak search and triangulation) was proposed, which can extract distinguishable airflow profile-related features (exhale area, inhale area, inhale/exhale speed, and breathing depth) for medium-scale experiments of 20 different participants to examine the feasibility of extraction of an individual's respiratory features from a combined mixture of motions for subjects. Independent component analysis with the joint approximation of diagonalization of eigenmatrices (ICA-JADE) algorithm was employed to isolate individual respiratory signatures from combined mixtures of breathing patterns. The extracted hyperfeature sets were then evaluated by integrating two different popular ML classifiers, k-nearest neighbor (KNN) and support vector machine (SVM), for subject authentication. Accuracies of 97.5% for two-subject experiments and 98.33% for single-subject experiments were achieved, which supersedes the performance of prior reported methods. The proposed identity authentication approach has several potential applications, including security/surveillance, the Internet-of-Things (IoT) applications, virtual reality, and health monitoring.

**Index Terms**—Dynamic segmentation, identity authentication, machine learning (ML) classifiers, radar, RF sensing.

Manuscript received 28 February 2022; revised 4 May 2022 and 31 May 2022; accepted 3 July 2022. This work was supported in part by the U.S. National Science Foundation (NSF) under Grant IIS1915738 and Grant CNS2039089. (Corresponding author: Shekh M. M. Islam.)

This work involved human subjects or animals in its research. Approval of all ethical and experimental procedures and protocols were granted by the University of Hawaii Human Studies Program's Institutional Review Board (IRB), and performed in line with the CHS# 14884 "Remote Sensing of Physiological Motion Using Doppler Radar" protocol.

Shekh M. M. Islam was with the Department of Electrical and Computer Engineering, University of Hawaii at Mānoa, Honolulu, HI 96822 USA. He is now with the Department of Electrical and Electronic Engineering, University of Dhaka, Dhaka 1000, Bangladesh (e-mail: shekh@hawaii.edu).

Olga Borić-Lubecke and Victor M. Lubecke are with the Department of Electrical and Computer Engineering, University of Hawaii at Mānoa, Honolulu, HI 96822 USA.

Color versions of one or more figures in this article are available at <https://doi.org/10.1109/TMTT.2022.3197413>.

Digital Object Identifier 10.1109/TMTT.2022.3197413

## I. INTRODUCTION

CONTINUOUS identity authentication has the potential to provide a high level of security throughout a login session by verifying the user identity continuously even long after initiation [1]. Traditional authentication systems require initial verification, typically either through a password or facial recognition, only at the start of the login session thus potentially allowing subsequent undesired access to personal information (e.g., social security, credit card, and bank account numbers) [2], [3], [4]. In 2018, more than two billion personal e-mails, social media accounts, home addresses, and social security numbers were illegally accessed due to the one-pass validation nature of traditional identity authentication systems [2], [3], [4]. A growing need has developed for more secure continuous user identity authentication systems for both government and private applications [1], [2], [3]. The airline and automotive industries are investing in new, secure, and unobtrusive continuous authentication methods to provide better security while simultaneously improving passenger experience by reducing the cumbersome nature of identity authentication procedures [5]. To be useful for continuous operation, authentication approaches must be both accurate and unobtrusive.

Existing biometric authentication methods based on fingerprint [6], [7], iris [8], vein [9], [10], [11], [12], and eye movement [13] require the intentional engagement of users with the authentication system. Behavioral biometrics have also been investigated for authentication, including the use of keystroke dynamics [14], [15] and gaze pattern [16]; however, users need to continuously type or stare at the screen to maintain authentication, which hampers practical usability. Other methods such as facial recognition, as used with Windows 10 Hello [17], offer limited promise as traditional cameras are hampered by opaque obstructions and inconsistent lighting, and such video imaging also incurs substantial signal processing overhead and introduces privacy-related concerns. Physiological biometric-based approaches, such as pulse response [18], electroencephalogram (EEG) [19], or breathing sounds [20], have also been investigated, but these methods are cumbersome to use, introducing intrusive limitations such as the need for direct contact between the sensor and body surfaces. Radar-based identity verification is gaining attention as it is a noncontact and unobtrusive way of recognizing people [21]. In addition,



individuals have different physical characteristics associated with lungs, rib cage, and abdominal muscle strength, which leads to distinct variations in breathing motion patterns [21]. A particular challenge for this approach is the isolation of radar reflections from two individuals that may be present within the radar field of view.

Diederichs *et al.* [22] utilized the 57–64-GHz millimeter-wave (mm-wave) frequency-modulated continuous-wave (FMCW) radar to recognize people from the RF signal backscattered by the subcutaneous tissue of the palm. Although the proposed method achieved noncontact identification with 98% accuracy, users had to bring their hands very close to the antenna. Rissacher and Galy [23] extracted heartbeat-related features (peak power spectral density) using 2.4-GHz continuous-wave (CW) radar to authenticate individuals. Similarly, Shi *et al.* [24] utilized 24-GHz CW radar to extract the heartbeat segment of four different participants with an accuracy of 94.6%. Rahman *et al.* [25] proposed a dynamic segmentation technique to identify six different participants with a 90% success rate from their respiratory patterns; however, when the inhale/exhale area ratio was close for different subjects false classifications could be introduced [26]. In addition, Lin *et al.* [1] tested the feasibility of radar-based identity authentication by extracting a fiducial descriptor that provides unique cardiac displacement information used to recognize subjects. Recently, another study demonstrated the efficacy of radar-based continuous identity authentication by utilizing a short-time Fourier transform (STFT) and deep convolutional neural network [27]. However, all reported results are based on recognizing people when only a single subject is within view of the radar. In home and office environments, there is often a high probability of the presence of two subjects in front of the radar sensor, which results in a combined mixture of breathing patterns captured simultaneously by the radar measurement, thus introducing a complex problem for individual monitoring [28]. In the most recent attempt, Huang *et al.* [29] demonstrated the feasibility of multiperson recognition by using 77-GHz FMCW radar integrating a deep neural network with an accuracy of 95.40%. However, in their experimental scenarios, they considered only three subjects at significantly different distances from the radar. When subjects are equidistant and at the same range bin of the radar, FMCW radar cannot isolate them, and thus, the proposed system is ineffective [28].

Isolating independent respiratory signatures for two equidistant subjects, as shown in Fig. 1, remains a critical challenge, which is an important part of the work reported here. Note that while it is possible to use the direction of arrival (DOA) to isolate RF reflections from well-spaced subjects [shown in Fig. 1(a)] at the edges of the beamwidth, entangled reflections from closely spaced subjects [shown in Fig. 1(b)] within the beamwidth cannot be isolated in this manner. In preliminary work, an algorithm using CW radar integrated with the independent component analysis with the joint approximation of diagonalization of eigenmatrices (ICA-JADE) algorithm [29] was proposed. The robustness of the ICA-JADE algorithm to isolate the respiratory signatures of two equidistant subjects was subsequently tested with varied breathing patterns [30].

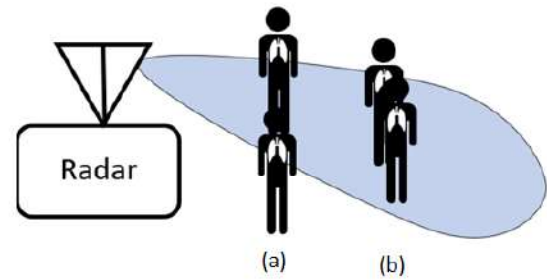


Fig. 1. CW radar system in a two-subject scenario with two equidistant subjects present within the beamwidth. (a) When well-separated subjects are located near the edges of the beamwidth, isolation of respiratory patterns is possible through DOA estimation. (b) When subjects are within the beamwidth (closely spaced), DOA estimation is not possible, and thus, the ICA-JADE algorithm is used to isolate the individual respiratory patterns from the combined mixture. From [28].

The ICA-JADE technique is adapted here to be effective in separating multiple respiratory signatures for continuous authentication of individuals, by integrating an iterative process that adjusts the crossover probability function to 0.5 from 0.001. A new approach to the dynamic segmentation algorithm is proposed here for extracting distinguishable features, and machine learning (ML) classifiers are also integrated to automatically recognize people from their breathing diversity. The feasibility and applicability for thus isolating and authenticating two equidistant subjects are tested and verified as well. Such noncontact radar systems have the potential to offer unobtrusive identity authentication in a manner that is suitable for real-world continuous authentication applications in home and office environments where two-subject scenarios are prevalent.

In this article, feasibility is tested for recognizing individuals when two equidistant subjects are present in front of the radar system. The core contribution is given as follows.

- 1) The ICA-JADE method of separating respiratory signatures was adapted by tuning the data-driven crossover probability parameter for use in authentication, by developing a more iterative process to incorporate more detailed information in the isolated respiratory patterns.
- 2) A new approach to the dynamic segmentation algorithm is proposed, which can extract highly distinguishable breathing-dynamic-related hyperfeatures (inhale area, exhale area, inhale/exhale speed, and breathing depth) and improve the accuracy of the system beyond prior reported results.
- 3) A hyperfeature set with two different popular classifiers, k-nearest neighbor (KNN) and support vector machine (SVM), is evaluated and shown to achieve promising performance both for single-subject and multisubject experimental scenarios.

A particular novelty of this work is the complete implementation of noncontact identity authentication for two equidistant subjects within a single radar antenna pattern. Currently published work on identity authentication is all based on the assumption that the received echoes are backscattered from a single person in the radar field of view. To the best of



our knowledge, this is the first attempt at recognizing two subjects concurrently within the beamwidth of the radar system. Our prior study on separation techniques (ICA-JADE and DOA) demonstrated better efficacy for isolating individual respiratory patterns in reflections from closely spaced subjects (within beamwidth) using the ICA-JADE method and DOA performs well for isolating respiratory patterns for well-spaced subjects (at the edge of the beamwidth) [28], [30], [31]. In this work, efficacy is examined by adapting the previously reported ICA-JADE approach to isolate the respiratory patterns from combined mixtures in order to accurately recognize two equidistant subjects within the beamwidth of the radar system, identifying individuals from a sample group of 20 subjects. In addition, a new approach to the dynamic segmentation algorithm was proposed here to extract reliable and unique breathing-dynamic-related features, which were then integrated with two popular ML classifiers to successfully enable continuous authentication for two individuals. Moreover, integrating ML classifiers with extracted radar-measured respiratory feature sets also demonstrates the power of ML in combination with distinct microwave signals, which can be of great interest to microwave researchers interested in applications that can benefit from the introduction of ML, such as automotive radar detection, object localization, and classification approaches.

The rest of this article is organized as follows. Section II discusses the theoretical background of respiration sensing in a multisubject environment, and Section III highlights the proposed noncontact identity authentication system. Section IV presents experimentation and validation, and Section V illustrates the results. Section VI concludes with a summary.

## II. THEORETICAL BACKGROUND

In this section, the theoretical background of the proposed identity authentication system is described. This includes the theoretical background of two equidistant subject measurements and the basics of the ICA-JADE algorithm.

### A. Multisubject Respiration Measurement and Separation

When there are two equidistant subjects present in front of the radar system, a combined mixture of respiration patterns is received, which is made up of signatures that are very difficult to separate [28], [30], [31]. RF reflections from two bodies become superimposed, which is a critical problem in practical real-world scenarios [31]. A CW radar has been used in respiration detection because of its high sensitivity for motion detection and simpler architecture than the FMCW radar [32]. It transmits a single-tone CW signal to the human body. When the radio wave is reflected by the chest wall, the respiratory and heartbeat information will be modulated into the CW signal in the form of a phase shift [32].

Suppose that there are two subjects present in front of a radar transceiver, as shown in Fig. 1. In a single-subject environment, the phase-modulated signal at a quadrature receiver

is given by [33]

$$B_I(t) = A_{BI} \cos\left(\frac{4\pi d_o}{\lambda} + \frac{4\pi x(t)}{\lambda} + \Delta\phi(t)\right) \quad (1)$$

$$B_Q(t) = A_{BQ} \sin\left(\frac{4\pi d_o}{\lambda} + \frac{4\pi x(t)}{\lambda} + \Delta\phi(t)\right) \quad (2)$$

where  $\theta$ ,  $\lambda$ ,  $\nabla\phi$ ,  $d_o$ , and  $x(t)$  represent the constant phase shift, wavelength, residual phase noise of the oscillator, distance from the receiving end, and distance of the movement of the abdomen, respectively [33]. In a multiple-subject environment, the received signal at the in-phase receiver is given by

$$\begin{aligned} B_{I1}(t) &= A_{BI} \cos\left(\frac{4\pi d_o}{\lambda} + \frac{4\pi x_1(t)}{\lambda} + \Delta\phi(t)\right) \\ B_{I2}(t) &= A_{BI} \cos\left(\frac{4\pi d_o}{\lambda} + \frac{4\pi x_2(t)}{\lambda} + \Delta\phi(t)\right) \\ B_{I3}(t) &= A_{BI} \cos\left(\frac{4\pi d_o}{\lambda} + \frac{4\pi x_3(t)}{\lambda} + \Delta\phi(t)\right) \\ B_{IN}(t) &= A_{BI} \cos\left(\frac{4\pi d_o}{\lambda} + \frac{4\pi x_n(t)}{\lambda} + \Delta\phi(t)\right). \end{aligned} \quad (3)$$

Similarly, for quadrature, the receiver is given by

$$\begin{aligned} B_{Q1}(t) &= A_{BQ} \sin\left(\frac{4\pi d_o}{\lambda} + \frac{4\pi x_1(t)}{\lambda} + \Delta\phi(t)\right) \\ B_{Q2}(t) &= A_{BQ} \sin\left(\frac{4\pi d_o}{\lambda} + \frac{4\pi x_2(t)}{\lambda} + \Delta\phi(t)\right) \\ B_{Q3}(t) &= A_{BQ} \sin\left(\frac{4\pi d_o}{\lambda} + \frac{4\pi x_3(t)}{\lambda} + \Delta\phi(t)\right) \\ B_{QN}(t) &= A_{BQ} \sin\left(\frac{4\pi d_o}{\lambda} + \frac{4\pi x_n(t)}{\lambda} + \Delta\phi(t)\right). \end{aligned} \quad (4)$$

In this particular scenario, suppose that the radar transceiver has one transmitter and two receivers, and two subjects present; thus,  $N = M = 2$ , where  $N$  is the number of subjects and  $M$  is the number of receivers. The received signal can be represented by

$$\begin{bmatrix} \text{Receiver}_1 \\ \text{Receiver}_2 \end{bmatrix} = \begin{bmatrix} a_{11} & a_{12} \\ a_{21} & a_{22} \end{bmatrix} \begin{bmatrix} B_{I1}(t) \\ B_{I2}(t) \end{bmatrix} + j \begin{bmatrix} a_{11} & a_{12} \\ a_{21} & a_{22} \end{bmatrix} \begin{bmatrix} B_{Q1}(t) \\ B_{Q2}(t) \end{bmatrix} \quad (5)$$

where  $a_{ij}$  are the mixing matrix parameters; in general,  $N = M = X$ , where  $X = 1, 2, 3, \dots, N$  can be represented as follows:

$$\begin{bmatrix} \text{Receiver}_1(t) \\ \text{Receiver}_2(t) \\ \vdots \\ \text{Receiver}_N(t) \end{bmatrix} = \begin{bmatrix} a_{11} & \cdots & a_{1N} \\ \vdots & \ddots & \vdots \\ a_{N1} & \cdots & a_{NN} \end{bmatrix} \begin{bmatrix} B_{I1}(t) \\ B_{I2}(t) \\ \vdots \\ B_{IN}(t) \end{bmatrix} + j \begin{bmatrix} a_{11} & \cdots & a_{1N} \\ \vdots & \ddots & \vdots \\ a_{N1} & \cdots & a_{NN} \end{bmatrix} \begin{bmatrix} B_{Q1}(t) \\ B_{Q2}(t) \\ \vdots \\ B_{QN}(t) \end{bmatrix}. \quad (6)$$

This formulation closely corresponds to a blind source separation (BSS) algorithm such as ICA-JADE. Our goal is to separate independent subject respiratory signatures from combined mixtures.



### B. BSS and Independent Component Analysis

The term “blind” illustrates the fact that: 1) the sensors are unaware of the source signals and 2) no other information is available about the source signals immediately beforehand. “Blindness” basically makes the process a versatile tool and promising for practical applications. Several BSS approaches have been proposed to correctly separate and isolate individual subject respiratory signatures from combined mixtures [34], [35]. The goal of BSS is to reconstruct a set of source signals from a set of mixtures, without knowing the properties of the sources and the mixing proportion [35]. If the sources are independent and have non-Gaussian distributions and the mixing is linear, one can recover the source signals from mixtures by using independent component analysis (ICA) [34], [35]. ICA is essentially a method for recovering individual signals from a mixture of signals. The underlying assumption is that each row of the data matrix is a weighted sum of different source signals. Suppose that two mixture signals  $z_1$  and  $z_2$  are linear combinations of two source signals. The linear mixtures can be written as

$$\begin{aligned} z_1 &= a_{11}s_1 + a_{12}s_2 \\ z_2 &= a_{21}s_1 + a_{22}s_2 \end{aligned} \quad A = \begin{bmatrix} a_{11} & a_{12} \\ a_{21} & a_{22} \end{bmatrix} S = \begin{bmatrix} s_1 \\ s_2 \end{bmatrix}$$

$$s_1 = \arctan\left(\frac{B_{Q1}(t)}{B_{I1}(t)}\right), \quad s_2 = \arctan\left(\frac{B_{Q2}(t)}{B_{I2}(t)}\right) \quad (7)$$

where  $A$  is the mixing matrix,  $S$  is the matrix of source signals, and  $s_1$  and  $s_2$  are the arc-tangent demodulated signals of different subjects. The objective of ICA is to find a separating matrix or demixing matrix  $W$ , where  $W = A^{-1}$ . Finally, the output signal can be represented as

$$s(t) = WZ. \quad (8)$$

In summary, ICA attempts to recover pure source signals by estimating a linear transformation using a criterion that measures statistical independence among the sources. This may be achieved using high-order statistics. There are different ICA algorithms available, among them fast ICA, Infomax, and the joint approximate diagonalization of eigenmatrices (JADE) which is the most popular [36]. JADE is a fourth-order statistics kurtosis-based ICA method [34]. The main advantage of this technique is that it is a matrix diagonalization-based approach, whereas other algorithms depend on optimization procedures, and hence, variable results may occur [34], [35], [36]. In prior reported results, the efficacy of the ICA-JADE algorithm was tested for separating respiratory signatures from a combined mixture of signals when subjects are closely spaced within the beamwidth [28], [30], [31]. In addition, the proposed system could also track and isolate the respiratory pattern of subjects when they were outside the beamwidth of the radar or at different distances, by utilizing DOA techniques [28], [37]. The system has a hybrid capability of isolating the respiratory patterns using ICA-JADE for closely spaced subjects and beam scanning (DOA) for well-spaced subjects [28]. For current interests, the more challenging scenario with two equidistant subjects within the radar beamwidth is of interest, so ICA-JADE is used. Performance measurements for well-spaced subjects are not described here because it is

expected that when subjects are well-spaced, the separation of independent respiratory signatures is less challenging due to multiple available options [28], [37] and thus beyond the scope of this article.

### III. NONCONTACT IDENTITY AUTHENTICATION SYSTEM

This section provides an overview of the proposed noncontact authentication system, and the remainder describes the associated hardware architecture.

#### A. System Overview

The proposed noncontact authentication system is based on the Doppler radar, which analyzes backscattered RF signals that carry body motion information indicating a human subject's vital signs (breathing rate and heart rate) and associated unique patterns [24], [26]. An additional advantage of this radar technique is that continuous authentication can be achieved without intrusive video imaging [25]. Reported prior results have focused solely on the use of respiratory motion to identify a single isolated subject [30]. Simultaneous measurement of two equidistant subjects within the beamwidth is a critical challenge [28]. While other proposed conventional biomedical radar-based identity authentication methods can only authenticate a single subject [1], [21], [24], [25], [26], the proposed technique adapts and incorporates the ICA-JADE algorithm to isolate individual respiratory patterns from a combined mixture even for concurrent measurement of two equidistant subjects with the field of view of radar. The proposed system can also track and recognize well-spaced subjects as described in prior reporting [29]. Fig. 2 shows the proposed unobtrusive identity authentication system. After isolating the respiratory patterns, distinguishable breathing-dynamic-related features are extracted, and then, ML classifiers are applied to authenticate recognized individuals. The main challenge, and thus the focus of this research, is the recognition of closely spaced subjects within the beamwidth of the radar transceiver.

#### B. Hardware Architecture

In the proposed authentication system, a 24-GHz KMC4 Monopulse radar transceiver with four different output channels ( $I_1$ ,  $I_2$ ,  $Q_1$ , and  $Q_2$ ) is employed [38]. Table I shows the hardware specification of the 24-GHz KMC4 Monopulse radar transceiver. The output channels were connected to four baseband amplifiers (Stanford Research System Model SR560). All the baseband amplifiers were ac-coupled with a gain of 200 and low-pass filtered with a cutoff frequency of 30 Hz. The four channels were connected to a data acquisition (DAQ) (NI DAQ 6009 series) with a sampling frequency of 100 Hz. A customized LABVIEW interface was used to capture all the signals. The complete setup is shown in Fig. 3. The 24-GHz KMC4 radar module can also estimate the DOA for well-spaced subjects [28], [31], [36]. One pair of channel signals ( $I1/Q1$ ) is sufficient for extracting the combined mixture of chest wall displacements through ICA-JADE-based arc-tangent demodulation, and this was carried out. For estimating



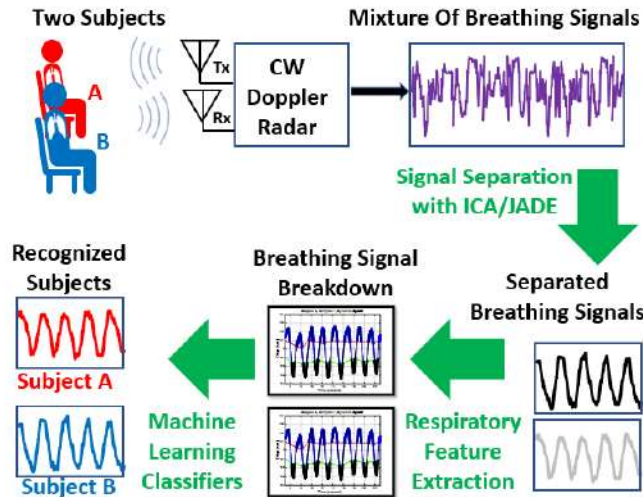


Fig. 2. Proposed noncontact identity authentication system for two-subject environments. The system can isolate the unique respiratory pattern for an individual from a combined mixture of signals. ML classifiers are also integrated with the system to recognize different participants from their extracted features.

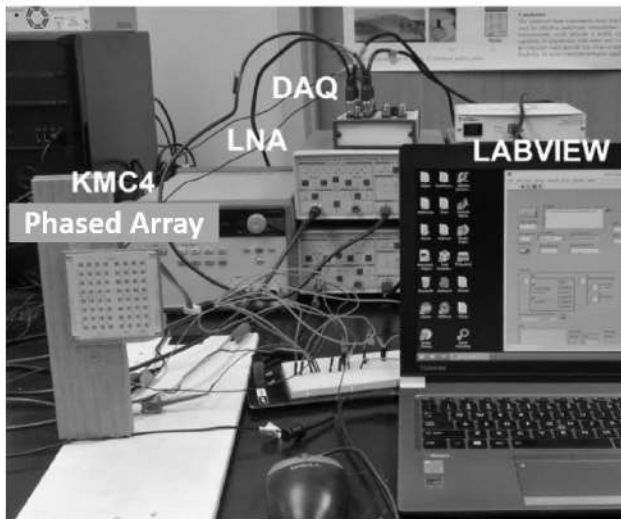


Fig. 3. Hardware architecture of the proposed noncontact continuous identity authentication system. The 24-GHz K-MC4 off-the-shelf radar has been integrated with a low-noise amplifier (LNA) and a DAQ system. A customized LABVIEW interface captures respiration patterns.

DOA, both pairs of channel signals would be required, but such DOA separation was not carried out in this experiment.

#### IV. EXPERIMENTATION AND EVALUATION

Experiments were conducted on 20 different participants to assess the efficacy of recognizing individual subjects by their radar-captured respiratory signatures. For each trial, two subjects each sat in front of a radar, 0.5–1 m away, with an angular discrimination limit between the two subjects of 0.4 m. Fig. 4 shows the experimental setup for data collection. The experimental procedure involving human subjects described in this article was approved by the University of Hawaii Institutional Review Board (IRB). Twenty subjects aged between

TABLE I  
DOPPLER RADAR SYSTEM SPECIFICATION

Parameter	Value
Antenna Array size	Transmitter: $1 \times 8$ patch array Receiver: $2 \times 8$ patch array
Center Frequency	24.25 GHz
Antenna gain	13.0 dBi
Beamwidth	E-plane: beamwidth $30^\circ$
Antenna power	18 dBm



Fig. 4. Human experiment setup in an anechoic chamber. Two subjects were seated 1 m away from the radar system and the angular discrimination limit between two subjects was around 0.4 m, so they were within the beamwidth of the radar. Chest belt was attached to the body, which acts as a reference respiration measurement.

16 and 35 participated in the study, over the course of two months. Their body weights were between 42 and 85 kg. None had any heart disease. During each trial, two subjects were randomly paired, asked to wear chest bands (UFI1132 piezoelectric respiration transducer), and seated in front of the radar system. Datasets were collected for about 2 min (120 s) for each trial and the collected dataset was a combined mixture of the respiration patterns of the two subjects. Therefore, in total, measurements were recorded 15 times for each different pair of participants on different days. Individual chest belts were used for capturing individual respiration patterns as a reference, with two chest belts directly connected to the DAQ. These isolated reference patterns allowed for testing the efficacy of the ICA-JADE algorithm. Before extracting hyper-features, the ICA-JADE algorithm was employed to isolate the



individual respiration pattern with the results compared with the individual reference chest belt measurements.

### A. Preprocessing of Radar-Captured Signals

After capturing the concurrent measurement signal for each pair of subjects using a 100-Hz sampling rate, the signals were digitally preprocessed. Each signal was filtered using an FIR low-pass filter of an order of 1000 with a cutoff frequency of 10 Hz, as the physiological information of interest (breathing rate and heart rate) was expected within that frequency bandwidth [25], [26], [27]. After filtering, the arc-tangent demodulation technique was used to find the combined mixture of chest wall displacements [25], [26]. Then the ICA-JADE method was employed to isolate respiratory signatures from the combined mixture of breathing patterns. Fig. 5 shows the isolated respiratory signatures and a comparison with chest belt reference measurements. After isolating the respiratory pattern, a low-pass filter with a cutoff frequency of 2 Hz was applied, and a fast Fourier transform (FFT) was used to extract breathing rate and heart rate information. Fig. 6 shows the breathing rate and heart rate of two subjects, extracted from separated respiratory signatures. Breathing rate and heart rate include overlapping harmonics. From Fig. 7, it can be seen that the breathing and heart rates of subjects 1 and 8 are 0.25, 0.98, 0.4, and 0.99 Hz. In this study, we found that with few exceptions, the breathing range was consistent across subjects. The normal breathing rate for an adult at rest is around 12–20 breath cycles per minute [25]. The respiratory rate may change from 12 to 25 breathing cycles per minute due to physical activities, stress, and other activities occurring just before radar measurements (such as walking upstairs). However, for most of the participants, breathing rates fell into overlapping ranges. For example, in Fig. 6(c) and (d), subjects 4 and 5 have quite similar breathing rates of 0.33 and 0.32 Hz, respectively. Therefore, extracting only breathing rate and heart rate cannot be a unique way to recognize an individual subject as subjects may have overlapping rates [25].

### B. Respiratory Feature Extraction

For extracting respiratory features, visible patterns in the time-domain representation of the separated respiratory signals were examined. Ten different respiratory features were extracted from the time-domain representation of the separated respiratory signals. Fig. 7 shows the extracted features used from the different experiment trials. The investigated features have been classified into two different spaces shown in Table II. One of them is typical features and another one is hyperfeatures. The typical respiratory feature extraction process is described in prior work [25], [39]. Among all the typical features, dynamic segmentation was the most dominant feature used to recognize people accurately with an accuracy of above 90% [39]. Simplistically, the breathing cycle can be segmented into four various episodes: inhale ramp up, the transition from inhale to exhale, exhale ramp down, and transition from exhaling to inhale [25]. The basic idea of dynamic segmentation is that it considers 30%–70% of the transition period ramp up and ramp down of both inhale and

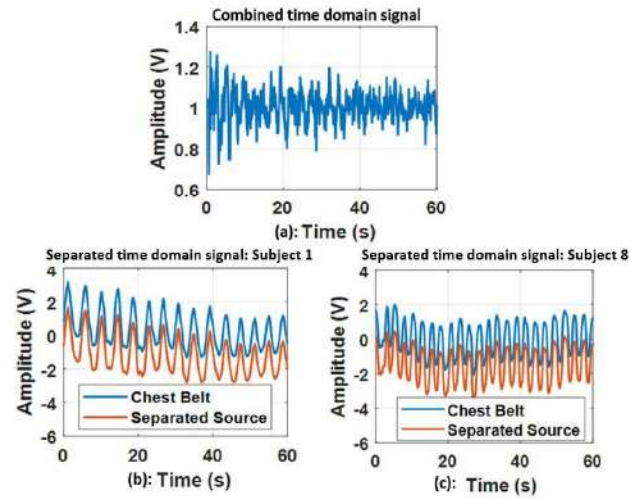


Fig. 5. Recorded combined mixture and separated signals for two subjects. While individual signals are not apparent in (a) combined mixture, individual respiratory patterns are apparent in the separated signals for subjects (b) 1 and (c) 8. Note that the blue lines represent the chest belt signals and the red lines represent the separated source signals.

exhale episodes and then calculates the displacement versus time area ratio of the episodes [25], [26], [39]. The area ratio is calculated based on the following equation:

$$R = \frac{\text{Area inhale to exhale trapezium}}{\text{Area exhale to inhale trapezium}} \quad (9)$$

$$= \left( \frac{1}{N} \right) * \sum_{i=1}^N \left( \frac{A_{\text{exi}}}{A_{\text{ini}}} \right) \quad (10)$$

where  $A_{\text{exi}}$  is the area of the transition from exhale to inhale,  $A_{\text{ini}}$  is the area of the transition from inhale to exhale, and  $N$  is the number of breathing cycles. This also indicates how one initiates the next cycle of breathing patterns [25]. Fig. 8 shows the dynamically segmented inhale and exhale area ratio for two participants. The drawback of dynamic segmentation is that when the inhale and exhale area ratio becomes similar among subjects, it cannot be used by itself to identify human subjects accurately and creates ambiguity in the system [26]. In addition, the method considered a 30%–70% segment, so it discarded the heart-based dynamic-related phenomena evident in the excluded peaks of the inhale and exhale transitions [39]. In a recent study, the robustness of the dynamic segmentation technique was tested on subjects after performing physiological activities (walking upstairs) where it was found that the breath ratio also changes notably with physiological activities [39]. Thus, a new, robust unique feature extraction algorithm is required for reliable and accurate noncontact identity authentication.

### C. Hyperfeature Space (Peak Search and Triangulation)

After separating independent respiratory signatures, a peak search method was used to find local maxima and minima points in that segmented portion of the signal. The 12.8-s window size was selected for the portion as it represented the minimum number of samples required for the FFT operation



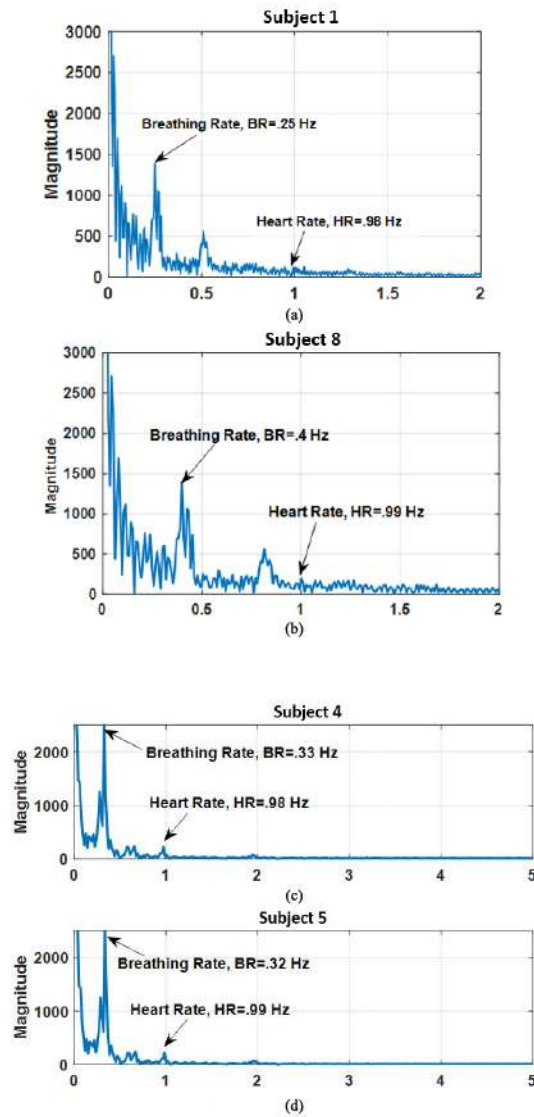


Fig. 6. Extracted breathing and heart rates from patterns isolated from combined mixtures. The breathing and heart rates of (a) subject 1 are 0.25 and 0.98 Hz and (b) subject 8 are 0.4 and 0.99 Hz. On the other hand, (c) subject 4 and (d) subject 5 have quite similar breathing rates of 0.33 and 0.32 Hz, respectively.

to extract the breathing and heart rates and it also contains at least two complete breathing cycles [26]. After finding the peaks of maxima and minima of the segmented portion of the signal, an array of two consecutive maxima and one minimum in-between point was created, and then, a triangle was constructed within those three points (two maxima and one minimum). After triangulation, the area of that triangle was calculated for the inhale and exhale episodes, and the average of the inhale and exhale areas within the window was calculated. Using triangulation, the inhale and exhale speed was calculated as one arm of the triangle, which represents the slope of the transition period (inhale and exhale). One of the advantages of including the peaks of the respiratory patterns in the proposed technique is that it integrates cardiac-based dynamics [1], [24]. The inhale and exhale areas represent two different cardiac phenomena. The inhale area represents

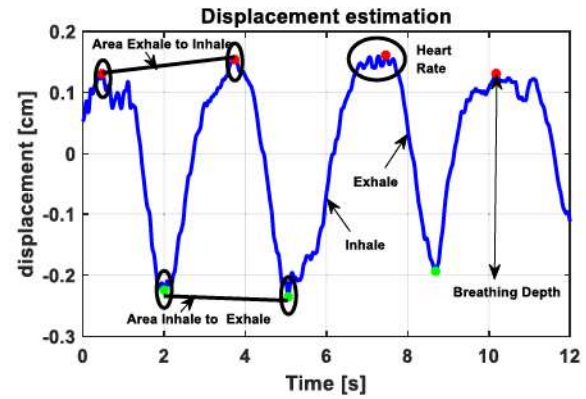


Fig. 7. Three complete cycles of respiration signal measured using a 24-GHz radar system. Each breathing cycle consists of inhale, exhale, and transition episodes. Ten different respiratory dynamic-related features were extracted and investigated for their identifiability and uniqueness.

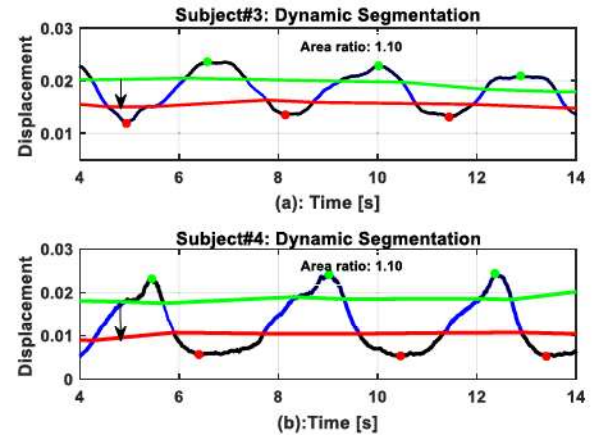


Fig. 8. Dynamically segmented inhale and exhale area ratio for (a) subject 3 and (b) subject 4. Note that they have equal area ratios of 1.10.

TABLE II  
EXTRACTED BREATHING DYNAMIC-RELATED FEATURES

Feature Space	Features
Typical features	<ul style="list-style-type: none"> <li>Breathing rate/heart rate</li> <li>Average exhale cycle period</li> <li>Standard deviation of exhale cycle period</li> <li>Average inhale cycle period</li> <li>Standard deviation of inhale/exhale cycle period</li> <li>Dynamic segmentation</li> </ul>
Hyper-features	<ul style="list-style-type: none"> <li>Exhale area</li> <li>Inhale area</li> <li>Inhale/exhale speed</li> <li>Breathing depth</li> </ul>

the ventricular filling state of the heart and the exhale area represents ventricular contraction [40]. During these stages, different people might have different breathing depth and



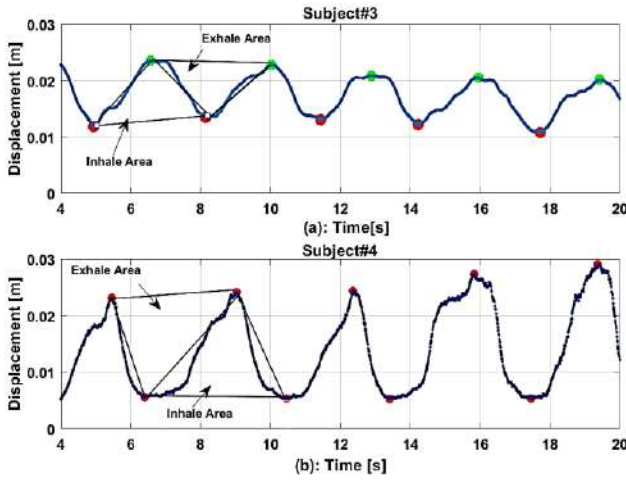


Fig. 9. Illustration of inhale and exhale areas of (a) subject #3 and (b) subject #4. There are clear visible differences in their inhale and exhale areas and speed patterns, even though their dynamically segmented area ratios were similar (shown in Fig. 8).

airflow profiles due to variations in cardiac movement, which will affect the area of that segment [1], [24], [40]. Fig. 9 shows that the inhale and exhale areas of the two participants are significantly different from their similar dynamically segmented inhale/exhale area ratios (shown in Fig. 8). From Fig. 9, the chest displacement of subject 4 can be seen to be slightly higher than that of subject 3. Calculating the triangle region helps to add variation in the inhale area and the exhale area as it takes into consideration two consecutive peak points (two minimum and one maximum point). Integrating the peak search process and triangulation method also helps to consider the breathing depth variations for calculating inhale and exhale areas. Dynamically segmented inhale and exhale area ratio changes were also studied for subjects after physiological activities [39]. The dynamic segmentation method ignores the heart-related dynamics because it considers only 30%–70% of the chest displacement [39]. Fig. 10 shows a summary of the proposed new version of the dynamic segmentation algorithm. The area ratio is calculated after using an improved version of the dynamic segmentation based on the following equation:

$$R = \frac{\text{Area inhale to exhale triangle}}{\text{Area exhale to inhale triangle}} \quad (11)$$

$$= \left( \frac{1}{N} \right) * \sum_{i=1}^N \left( \frac{A_{\text{exi}}}{A_{\text{ini}}} \right). \quad (12)$$

## V. RESULTS

In this section, the accuracy of ML classifiers with hyperfeature sets is described. A comparative analysis of the proposed technique with literature results is also described along with associated challenges of this technology for real-world implementation.

### A. Respiratory Dynamic-Related Feature

The feature extraction process was described in Section IV. Two subjects with a similar physique were (otherwise)

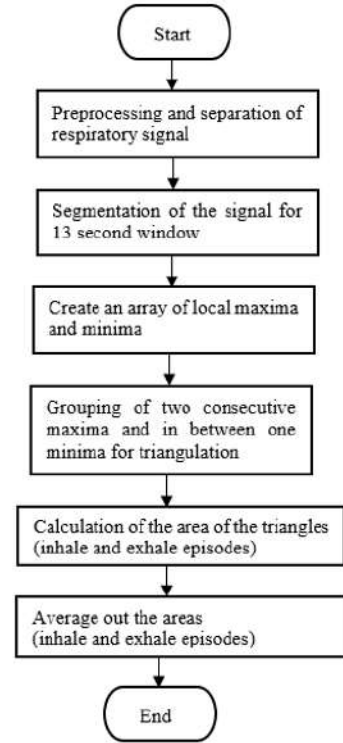


Fig. 10. Summary of the new algorithm (flowchart) used for determining the inhale and exhale areas, and speed.

randomly paired and arranged in a seated position in front of the radar system. Experiments were performed both in an anechoic chamber and in an ordinary office environment. For each paired subject's experiment, 15 measurements were taken within a 120-s window, where measurements were divided into 12.8-s segments. Before segmentation, the ICA-JADE algorithm was employed to isolate the respiratory patterns [28], [30], [31]. Respiratory features for the 12.8-s windows were then extracted. The window is long enough to extract breathing and heart-rate-related information as the FFT window size is around 128, and thus, almost 12 800 samples are required, which establishes the minimum window resolution limit [26]. These hyperfeature datasets were used to perform classification and person identification. Ten features were extracted and four of them were found to be much more dominant in terms of their uniqueness, so they were considered hyperfeatures. Fig. 11 shows the extracted hyperfeatures for six different participants. Inhale area, exhale area, breathing depth, and inhale/exhale speed are the four dominant unique features that were significantly different for participants.

### B. ML Classifiers

After extracting unique features, 2/3 of the dataset was used for training and 1/3 of the dataset was used for testing the performance of ML classifiers. Therefore, in total, there were 30 sets of data for each participant containing almost 1 min of recordings. The KNN and SVM classifiers were integrated for recognizing people from their extracted respiratory dynamic-related hyperfeatures. KNN and SVM have supervised classification tools [41]. KNN is based on clustering elements that



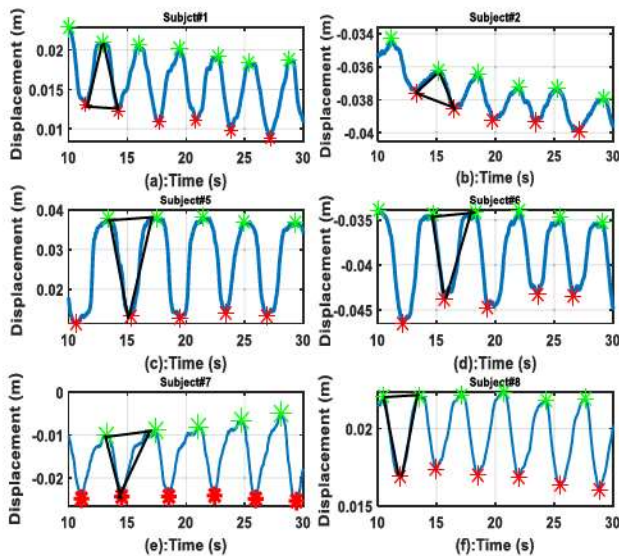


Fig. 11. Extracted respiratory features for six different participants: (a) subject 1, (b) subject 2, (c) subject 5, (d) subject 6, (e) subject 7, and (f) subject 8. While the respiratory traces all show a periodic pattern, the extracted hyperfeatures (inhale area, exhale area, inhale/exhale speed, and breathing depth) differ significantly between subjects. Subject#5 clearly has higher inhale and exhale areas than other participants.

TABLE III  
EXTRACTED BREATHING DYNAMIC-RELATED FEATURES

CLASSIFIER	ACCURACY
KNN (CUBIC)	84.4%
KNN (COSINE)	86.4%
KNN (MEDIUM)	86.9%
SVM (LINEAR)	95%
SVM (QUADRATIC)	97.5%
SVM (FINE GAUSSIAN)	93.5%
SVM (MEDIUM GAUSSIAN)	96.5%

try to find the nearest neighboring elements [41]. SVM is a hyperplane-based classification approach [42]. Different kernel functions were integrated for both KNN and SVM to test the accuracy of the system [43]. Table III shows the different ML classifier accuracies achieved for recognizing human subjects. A fivefold cross-validation model was also used for training the classifiers. Among all classifiers, SVM with a quadratic function outperformed the others with an accuracy of 97.5%. Fig. 12 shows the confusion matrix of SVM with quadratic function classifiers to recognize different subjects based on their extracted respiratory hyperfeatures. From the confusion matrix, it is shown that subject 2 was misclassified as subject 1 for 5% of attempts, subject 3 was misclassified as subject 4 for 9%, subject 4 was also misclassified as subject 5 for 5%, and subject 7 was similarly misclassified as subject 6 for 14%. Misclassification occurred due to overlapping inhale and exhale areas of the subjects. Misclassification occurs between adjacent subjects due to the placement of the feature vector of misclassified subjects one after another before feeding them into the ML classifier. The rest of the subject characteristics were classified accurately, and the overall classification accu-

racy was 97.5%, which provides a clear indication of the efficacy of the proposed method and experimental system. The learning curve of the outperforming SVM classifier with a quadratic function was also examined. Fig. 13 shows the learning curve of SVM with a quadratic function. With an increase in training sequences, the gap between the training score and the cross-validation score decreases, indicating that the training model has less variance and bias. After 60 training sequences, the two curves closely overlap, which reduces the gap between the two graphs. While adding more training instances can increase the training score of the learning algorithm, the comparison shown indicates a reasonable accuracy of 97.5% within 60 training sequences. The proposed system and algorithm can identify two subjects simultaneously after isolating the respiratory patterns from the combined mixture of breathing.

### C. Comparative Analysis Between the Proposed Method and Reports in the Existing Literature

An accuracy comparison was performed between the proposed method and those in the existing literature. In a prior study, the dynamic segmentation technique and its efficacy were reported to accurately recognize people for single-subject experimental scenarios [25]. This experiment was performed on six different participants. The same experimental dataset in [25] was used with the proposed improved version of the dynamic segmentation approach (peak search and triangulation) to compare accuracies. The training dataset for single subject and multisubject to test the accuracy of ML classifiers is completely different as the single-subject dataset was taken from our prior published work in [25]. Fig. 14 shows the confusion matrix of six different participants using the improved version of the dynamic segmentation technique and the previous dynamic segmentation technique for feature extraction. In the prior study, a 2.4-GHz radar system was used and six different participants were measured on different days of the week [25]. Fifteen sets of 60-s respiration traces were collected with a 100-Hz sampling rate [25]. All experiments were performed with a single subject present in front of the radar system [25]. Breathing ratio features were extracted using previously reported dynamic segmentation techniques. In addition, the inhale area, exhale area, inhale/exhale speed, and breathing depth were extracted using the improved version of the dynamic segmentation technique. SVM with quadratic function outperformed for both scenarios. Fig. 14 shows that subject 1 was misclassified in 40% of the cases using the original dynamic segmentation technique, whereas the improved version of the feature extraction technique reduced the misclassification rate by 10%. The classification accuracy using the dynamic segmentation technique was almost 93.33%, whereas using the new method classification accuracy improved to 98.33% for the previously reported dataset [25].

An accuracy comparison was also performed between the proposed improved version of the dynamic segmentation method and existing methods reported in the literature. Table IV shows the comparative analysis of this work with the existing literature. Previously reported results used 2.4-GHz



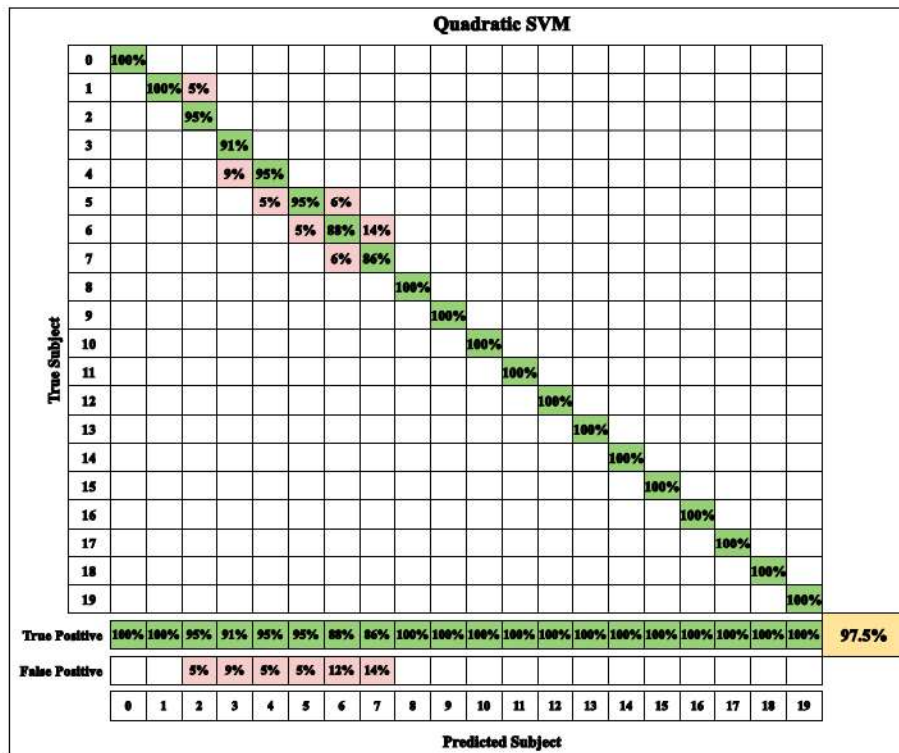


Fig. 12. Confusion matrix showing the true- and false-positive rates of 20 different participants. Thirty sets of 12.8-s windows for combined mixture data were taken as a feature set for each participant. The overall classification accuracy was calculated based on the average of true-positive rates of different participants, which was almost 97.5%.

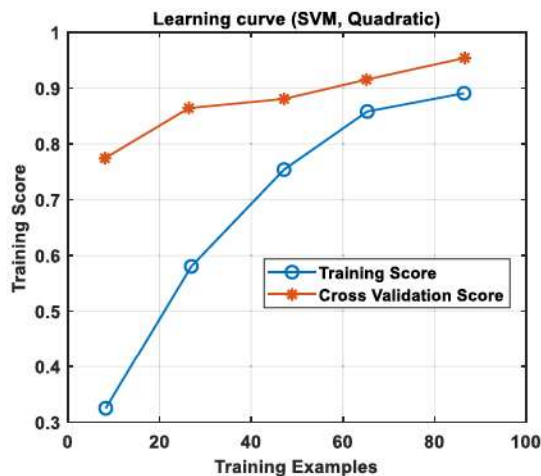


Fig. 13. Learning curve of SVM with a quadratic function. With an increase in training sequences, the training score closely matches the cross-validation score. The training score does not overlap or cross the validation score, so there is no overfitting incidence in the training sequences.

CW radar, and for extracting unique features, they used heart-related fiducial-based descriptors. The accuracy of the described system was 98.61% [1]. In addition, other attempts also showed an accuracy of 98% by utilizing an STFT of the radar-captured heartbeat waveform pattern variation [27]. For the experimental scenario with at least two subjects in view, the performance may degrade from the reported results [28]. The system proposed here showed efficacy for recognizing people in a single-subject experimental scenario

with an accuracy of 98.33%. Moreover, the integration of the ICA-JADE algorithm in the proposed system facilitated the use of this system in the presence of two subjects with an accuracy of 97.5%. The deep learning approach was not integrated with the proposed system because the ML approach helps to extract unique respiratory features, while the deep learning approach is mostly used for automatic feature extraction. However, the performance of the proposed ML-based approach was compared with published deep learning-based approaches such as deep convolutional neural network, which was integrated with micro-Doppler signatures in prior reported attempts [27], [29]. The proposed improved dynamics segmentation algorithm with an ML-based approach shows reasonable accuracy compared to the deep learning-based approach, as shown in Table IV.

The proposed system was mostly tested for sedentary respiration patterns because meaningful identifying breathing parameters occur mainly during the sedentary condition, as opposed to activity-dependent patterns that occur during arbitrary activity. Sedentary conditions occur quite commonly and thus provide a consistent basis for comparative respiratory monitoring [44]. Daily variations of sedentary breathing patterns were also considered over the approximately two-month-long studies. In addition, the efficacy of the proposed system was also tested with six different participants after short periods of exertion (walking upstairs) with an accuracy of above 90%, and aerobic dynamics related to unique features (exhale area and inhale area) tended to change for patterns in a consistent manner [39]. Identification error increases with an increase in overlap of sedentary classifiers, and thus, “learning”



TABLE IV  
COMPARISON OF THIS ARTICLE WITH OTHER RECENT RELEVANT WORKS

REFERENCE & YEAR	RADAR TYPE & FREQ (GHz)	SUBJECT IN RADAR VIEW	NUMBER OF SUBJECT	FEATURE EXTRACTION ALGORITHM	ACCURACY (%)
[1] 2017	CW 2.4 GHz	1	78	HEART-BASED DYNAMICS (FIDUCIAL BASED DESCRIPTOR FIVE POINTS)	98.61%
[24] 2018	CW 24 GHz	1	4	HEAR TBEAT SIGNAL COMPLEXITY	94.6%
[25] 2018	CW 2.4 GHz	1	6	DYNAMIC SEGMENTATION (AREA RATIO)	93.33%
[27] 2020	CW 24 GHz	1	10	SHORT-TIME FOURIER TRANSFORM (HEARTBEAT, ENERGY AND BANDWIDTH)	98.5%
THIS WORK FOR SINGLE SUBJECT	CW 24 GHz (DATASET OF REFERENCE [25])	1	6	IMPROVED VERSION OF DYNAMIC SEGMENTATION (INHALE AREA, EXHALE AREA, BREATHING DEPTH)	98.33%
[29] 2020	FMCW 77 GHz	2	3	MICRO-DOPPLER SPECTROGRAM WITH DEEP NEURAL NETWORK	95.40%
THIS WORK FOR MULTI-SUBJECT	CW 24 GHz	2	20	IMPROVED VERSION OF DYNAMIC SEGMENTATION (INHALE AREA, EXHALE AREA, BREATHING DEPTH)	97.5%

how activity affects an individual can offset this error to maintain a high efficacy rate of identification [39]. Moreover, in prior work, the proposed system also showed efficacy to recognize people with breathing disorders such as obstructive sleep apnea (OSA) with an accuracy of above 90% [45]. Therefore, the initial feasibility of the reliable accuracy of the proposed system was tested in realistic scenarios such as after short exertions and with OSA symptoms. Further feasibility tests of the proposed identity authentication system in realistic settings remain an active investigation.

#### D. Challenges for Noncontact Identity Authentication

A major challenge for radar-based noncontact continuous identity authentication is the management of the motion artifacts produced by random body movement and the presence of extraneous subjects [21]. All reported results rely on the recognition and exploitation of a controlled environment for analyzing periods of sedentary physiological motion [21]. None of the attempts in the literature have focused on recognizing people when they are equidistant from the radar and within the field of view [1], [21], [24], [25], [27]. In this

particular work, the feasibility of recognizing individuals when two subjects are in the radar field of view was demonstrated. Prior research also demonstrated the efficacy of Doppler radar respiration sensing during random body movement [46], [47], [48]. A Doppler radar sensor with camera-aided random body movement cancellation has also been demonstrated in prior research [46]. In the associated methodology, random body movement can be mitigated in three different ways, such as using phase compensation at the Doppler RF front end [48], phase compensation for the baseband complex signal [47], and cancellation within the demodulation technique [46]. In prior work, the efficacy of an adaptive filter technique was demonstrated for compensating platform motion for an unmanned aerial vehicle (UAV) radar system used to extract vital signs [49]. Potentially, in future work, methods like these can be integrated with the authentication system proposed here to mitigate the motion of random body movement.

Another challenge for noncontact identity authentication is the change in respiratory patterns caused by emotional stress and physical activity [40]. Breathing is controlled by a central neural mechanism, so the cardiopulmonary pattern may change with emotional and physical stress [40]. This work



Improved Version of Dynamic Segmentation (Quadratic SVM)							
True Subject	Sub 0	Sub 1	Sub 2	Sub 3	Sub 4	Sub 5	Overall
	60%	10%			20%	10%	
		100%					
			100%				
				100%			
					100%		
						100%	
							98.3%
Predicted Subject							

(a)

Dynamic Segmentation (Quadratic SVM)							
True Subject	Sub 0	Sub 1	Sub 2	Sub 3	Sub 4	Sub 5	Overall
	90%	10%					
		100%					
			100%				
				100%			
					100%		
						100%	
							98.3%
Predicted Subject							

(b)

Fig. 14. Confusion matrix of SVM with a quadratic function using (a) newly proposed version of dynamic segmentation technique and (b) original dynamic segmentation technique for classifying six different participants. The accuracy improved with the new technique.

focused on sedentary breathing patterns to test the feasibility of respiration-based sensing technologies to recognize people. Methods have been demonstrated for recognizing sedentary situations and restricting measurements to those intervals, which turns out to happen frequently [50]. Recognition of people with full accommodation of the variability of respiratory patterns due to emotion and physical stresses would be a large step beyond the scope of this article. However, the feasibility of isolating respiratory signatures using the ICA-JADE algorithm for varied breathing patterns in post-activity scenarios has been established in preliminary work [30].

Authentication time or latency is another important challenge for recognizing people using microwave Doppler radar. Generally, an authentication system should not only accurately identify people but also identify them with low latency [1].

For the system proposed here, a 12.8-s window is required to accurately recognize people. When the window size is less than 12.8 s, the accuracy of the system degrades due to the smaller number of breathing cycles present in the radar-captured pattern. Reducing accurate authentication to the time for one or fewer breaths is beyond the scope of this feasibility demonstration.

This present study demonstrates the feasibility of authenticating two subjects simultaneously in front of a radar system and authentication of more than two subjects at a time remains future work. In addition, in recent literature, a digital beamforming technique based on single-input-multiple-output (SIMO) radar has also been demonstrated to isolate individual respiratory patterns from the combined respiratory patterns for three closely spaced subjects [51]. Moreover, the underdetermined blind source separation technique (UBSS) has also demonstrated the feasibility of isolating respiratory patterns for three subjects from the combined radar-captured respiration patterns [52]. Thus, integrating those approaches into this authentication system proposed here remains a logical next step for further exploration of noncontact identity authentication for situations where more than two subjects are present.

## VI. CONCLUSION

This article proposes an improved version of the dynamic segmentation algorithm for recognizing people when two subjects are in the radar field of view and is the first reported investigation demonstrating noncontact identity authentication in equidistant two-subject scenarios using CW radar. Experimental results also demonstrate the efficacy of the improved version of the algorithm for extracting highly distinguishable cardiopulmonary dynamic-related features (exhale area, inhale area, inhale/exhale speed, and breathing depth). Extracted hyperfeature sets are also integrated with the ML classifiers (KNN and SVM). SVM with quadratic kernel outperformed other classifiers with an accuracy of 98.33% and 97.5% for single- and two-subject experiments, respectively. The results also demonstrate the initial efficacy of the proposed identity authentication approach and the potential improvement over traditional system vulnerabilities. While this work demonstrates the efficacy of this technology for functioning in the presence of two equidistant subjects in the field of view of the radar, a major hurdle for practical authentication applications, other challenges for human identification remain for the radar research community in addressing complications from further subject physical variations, physiological activities, and random body movement.

## REFERENCES

- [1] F. Lin, C. Song, Y. Zhuang, W. Xu, C. Li, and K. Ren, "Cardiac scan: A non-contact and continuous heart-based user authentication system," in *Proc. 23rd Annu. Int. Conf. Mobile Comput. Netw.*, Snowbird, UT, USA, Oct. 2017, pp. 315–328, doi: [10.1145/3117811.3117839](https://doi.org/10.1145/3117811.3117839).
- [2] Chaos Computer Club (CCC). (Sep. 2013). *Chaos Computer Club Breaks Apple-Touch ID*. Accessed: Nov. 10, 2016. [Online]. Available: <https://www.ccc.den>
- [3] Chaos Computer Club (CCC). (Dec. 2014). *Fingerprint Biometrics Hacked Again*. Accessed: Nov. 10, 2016. [Online]. Available: <https://www.ccc.den>



- [4] Z. Whittaker. *These Companies Lost Your Data in 2015 Biggest hacks and Breaches*. Accessed: Aug. 2016. [Online]. Available: <http://www.zdnet.com>
- [5] Accessed: Feb. 1, 2022. [Online]. Available: <https://www.biometricupdate.com/201803/airlines-and-airports-investing-in-biometrics-to-meet-growing-identity-check-demand>
- [6] C. Kauba and A. Uhl, "Fingerprint recognition under the influence of image sensor ageing," *IET Biometrics*, vol. 6, no. 4, pp. 245–255, Jul. 2017, doi: [10.1049/iet-bmt.2016.0106](https://doi.org/10.1049/iet-bmt.2016.0106).
- [7] J. Wang and G. Wang, "Quality-specific hand vein recognition system," *IEEE Trans. Inf. Forensics Security*, vol. 12, no. 11, pp. 2599–2610, Nov. 2017, doi: [10.1109/TIFS.2017.2713340](https://doi.org/10.1109/TIFS.2017.2713340).
- [8] F. Jiu, K. Noronha, and D. Jayaswal, "Biometric identification through detection of retinal vasculature," in *Proc. IEEE 1st Int. Conf. Power Electron., Intell. Control Energy Syst. (ICPEICES)*, New Delhi, India, Jul. 2016, pp. 1–5, doi: [10.1109/ICPEICES.2016.7853731](https://doi.org/10.1109/ICPEICES.2016.7853731).
- [9] Y. Wang, Y. Fan, W. Liao, K. Li, L.-K. Shark, and M. R. Varley, "Hand vein recognition based on multiple keypoints sets," in *Proc. 5th IAPR Int. Conf. Biometrics (ICB)*, New Delhi, India, Mar. 2012, pp. 367–371, doi: [10.1109/ICB.2012.6199778](https://doi.org/10.1109/ICB.2012.6199778).
- [10] D. Huang, Y. Tang, Y. Wang, L. Chen, and Y. Wang, "Hand-dorsa vein recognition by matching local features of multisource keypoints," *IEEE Trans. Cybern.*, vol. 45, no. 9, pp. 1823–1837, Sep. 2015, doi: [10.1109/TCYB.2014.2360894](https://doi.org/10.1109/TCYB.2014.2360894).
- [11] W. Kang and Q. Wu, "Contactless palm vein recognition using a mutual foreground-based local binary pattern," *IEEE Trans. Inf. Forensics Security*, vol. 9, no. 11, pp. 1974–1985, Nov. 2014, doi: [10.1109/TIFS.2014.2361020](https://doi.org/10.1109/TIFS.2014.2361020).
- [12] S. Veluchamy and L. R. Karlmarx, "System for multimodal biometric recognition based on finger knuckle and finger vein using feature-level fusion and K-support vector machine classifier," *IET Biometrics*, vol. 6, no. 3, pp. 232–242, May 2017, doi: [10.1049/iet-bmt.2016.0112](https://doi.org/10.1049/iet-bmt.2016.0112).
- [13] A. V. Lyamin and E. N. Cherepovskaya, "An approach to biometric identification by using low-frequency eye tracker," *IEEE Trans. Inf. Forensics Security*, vol. 12, no. 4, pp. 881–891, Apr. 2017, doi: [10.1109/TIFS.2016.2639342](https://doi.org/10.1109/TIFS.2016.2639342).
- [14] P. Pinto, B. Patrão, and H. Santos, "Free typed text using keystroke dynamics for continuous authentication," in *Communications and Multimedia Security (Lecture Notes in Computer Science)*, vol. 7908, C. Salinesi, M. C. Norrie, and O. Pastor, Eds. Berlin, Germany: Springer, 2014, pp. 33–45.
- [15] S. J. Shepherd, "Continuous authentication by analysis of keyboard typing characteristics," in *Proc. Eur. Conf. Secur. Detection*, Brighton, U.K., 1995, pp. 111–114, doi: [10.1049/cp:19950480](https://doi.org/10.1049/cp:19950480).
- [16] K. Mock, B. Hoanca, J. Weaver, and M. Milton, "Real-time continuous iris recognition for authentication using an eye tracker," in *Proc. ACM Conf. Comput. Commun. Secur. (CCS)*, Raleigh, NC, USA, 2012, p. 1007, doi: [10.1145/2382196.2382307](https://doi.org/10.1145/2382196.2382307).
- [17] J. Belifore. (Mar. 2015). *Making Windows 10 More Personal and More Secure*. Accessed: Mar. 10, 2017. [Online]. Available: <https://blogs.window.com/windowexperience/2015/03/17/making-windows-10-more-secure-with-windows-hello/#tKBXz8oqEQBUXG4q.97>
- [18] I. Martinovic, K. Rasmussen, M. Roeschlin, and G. Tsudik, "Authentication using pulse-response biometrics," *Commun. ACM*, vol. 60, no. 2, pp. 108–115, Jan. 2017, doi: [10.1145/3023359](https://doi.org/10.1145/3023359).
- [19] R. Das, E. Maiorana, and P. Campisi, "Visually evoked potential for EEG biometrics using convolutional neural network," in *Proc. 25th Eur. Signal Process. Conf. (EUSIPCO)*, Kos, Greece, Aug. 2017, pp. 951–955, doi: [10.23919/EUSIPCO.2017.8081348](https://doi.org/10.23919/EUSIPCO.2017.8081348).
- [20] L. Lu, L. Liu, M. J. Hussain, and Y. Liu, "I sense you by breath: Speaker recognition via breath biometrics," *IEEE Trans. Dependable Secure Comput.*, vol. 17, no. 2, pp. 306–319, Mar. 2020, doi: [10.1109/TDSC.2017.2767587](https://doi.org/10.1109/TDSC.2017.2767587).
- [21] S. M. M. Islam, O. Boric-Lubecke, Y. Zheng, and V. M. Lubecke, "Radar-based non-contact continuous identity authentication," *Remote Sens.*, vol. 12, no. 14, p. 2279, Jul. 2020, doi: [10.3390/rs12142279](https://doi.org/10.3390/rs12142279).
- [22] K. Diederichs, A. Qiu, and G. Shaker, "Wireless biometric individual identification utilizing millimeter waves," *IEEE Sensors Lett.*, vol. 1, no. 1, pp. 1–4, Feb. 2017, doi: [10.1109/LSSENS.2017.2673551](https://doi.org/10.1109/LSSENS.2017.2673551).
- [23] D. Rissacher and D. Galy, "Cardiac radar for biometric identification using nearest neighbour of continuous wavelet transform peaks," in *Proc. IEEE Int. Conf. Identity, Secur. Behav. Anal. (ISBA)*, Hong Kong, Mar. 2015, pp. 1–6, doi: [10.1109/ISBA.2015.7126356](https://doi.org/10.1109/ISBA.2015.7126356).
- [24] K. Shi, C. Will, R. Weigel, and A. Koelpin, "Contactless person identification using cardiac radar signals," in *Proc. IEEE Int. Instrum. Meas. Technol. Conf. (I2MTC)*, Houston, TX, USA, May 2018, pp. 1–6, doi: [10.1109/I2MTC.2018.8409645](https://doi.org/10.1109/I2MTC.2018.8409645).
- [25] A. Ragman, V. M. Lubecke, O. Boric-Lubecke, J. H. Prins, and T. Sakamoto, "Doppler radar techniques for accurate respiration characterization and subject identification," *IEEE J. Emerg. Sel. Topics Circuits Syst.*, vol. 8, no. 2, pp. 350–359, Jun. 2018, doi: [10.1109/JETCAS.2018.2818181](https://doi.org/10.1109/JETCAS.2018.2818181).
- [26] S. M. M. Islam, A. Rahman, N. Prasad, O. Boric-Lubecke, and V. M. Lubecke, "Identity authentication system using a support vector machine (SVM) on radar respiration measurements," in *Proc. 93rd ARFTG Microw. Meas. Conf. (ARFTG)*, Boston, MA, USA, Jun. 2019, pp. 1–5, doi: [10.1109/ARFTG.2019.8739240](https://doi.org/10.1109/ARFTG.2019.8739240).
- [27] P. Cao, W. Xia, and Y. Li, "Heart ID: Human identification based on radar micro-Doppler signatures of the heart using deep learning," *Remote Sens.*, vol. 11, no. 10, p. 1220, May 2019, doi: [10.3390/rs11101220](https://doi.org/10.3390/rs11101220).
- [28] S. M. M. Islam, O. Boric-Lubecke, and V. M. Lubecke, "Concurrent respiration monitoring of multiple subjects by phase-comparison monopulse radar using independent component analysis (ICA) with JADE algorithm and direction of arrival (DOA)," *IEEE Access*, vol. 8, pp. 73558–73569, 2020, doi: [10.1109/ACCESS.2020.2988038](https://doi.org/10.1109/ACCESS.2020.2988038).
- [29] X. Huang, J. Ding, D. Liang, and L. Wen, "Multi-person recognition using separated micro-Doppler signatures," *IEEE Sensors J.*, vol. 20, no. 12, pp. 6605–6611, Jun. 2020, doi: [10.1109/JSEN.2020.2977170](https://doi.org/10.1109/JSEN.2020.2977170).
- [30] S. M. M. Islam and V. M. Lubecke, "Extracting individual respiratory signatures from combined multi-subject mixtures with varied breathing pattern using independent component analysis with the JADE algorithm," in *Proc. IEEE Asia-Pacific Microw. Conf. (APMC)*, Hong Kong, Dec. 2020.
- [31] S. M. M. Islam, E. Yavari, A. Rahman, V. M. Lubecke, and O. Boric-Lubecke, "Separation of respiratory signatures for multiple subjects using independent component analysis with the JADE algorithm," in *Proc. 40th Annu. Int. Conf. IEEE Eng. Med. Biol. Soc. (EMBC)*, Honolulu, HI, USA, Jul. 2018, pp. 1234–1237, doi: [10.1109/EMBC.2018.8512583](https://doi.org/10.1109/EMBC.2018.8512583).
- [32] C. Li, V. M. Lubecke, O. Boric-Lubecke, and J. Lin, "A review on recent advances in Doppler radar sensors for noncontact healthcare monitoring," *IEEE Trans. Microw. Theory Techn.*, vol. 61, no. 5, pp. 2046–2060, May 2013, doi: [10.1109/TMTT.2013.2256924](https://doi.org/10.1109/TMTT.2013.2256924).
- [33] B. Park, O. Boric-Lubecke, and V. M. Lubecke, "Arctangent demodulation with DC offset compensation in quadrature Doppler radar receiver systems," *IEEE Trans. Microw. Theory Techn.*, vol. 55, no. 5, pp. 1073–1079, Jun. 2007, doi: [10.1109/TMTT.2007.895653](https://doi.org/10.1109/TMTT.2007.895653).
- [34] J.-F. Cardoso, "Blind signal separation: Statistical principles," *Proc. IEEE*, vol. 86, no. 10, pp. 2009–2025, Oct. 1998, doi: [10.1109/5.720250](https://doi.org/10.1109/5.720250).
- [35] L. De Lathauwer, B. De Moor, and J. Vandewalle, "Independent component analysis based on higher-order statistics only," in *Proc. 8th Workshop Stat. Signal Array Process.*, Corfu, Greece, Jun. 1996, pp. 356–359, doi: [10.1109/SSAP.1996.534890](https://doi.org/10.1109/SSAP.1996.534890).
- [36] D. N. Rutledge and D. Jouan-Rimbaud Bouveresse, "Independent components analysis with the JADE algorithm," *TrAC Trends Anal. Chem.*, vol. 50, pp. 22–32, Oct. 2013, doi: [10.1016/j.trac.2013.03.013](https://doi.org/10.1016/j.trac.2013.03.013).
- [37] S. M. M. Islam, E. Yavari, A. Rahman, V. M. Lubecke, and O. Boric-Lubecke, "Direction of arrival estimation of physiological signals of multiple subjects using phase comparison monopulse radar," in *Proc. Asia-Pacific Microw. Conf. (APMC)*, Kyoto, Japan, Nov. 2018, pp. 411–413, doi: [10.23919/APMC.2018.8617539](https://doi.org/10.23919/APMC.2018.8617539).
- [38] Accessed: Feb. 1, 2022. [Online]. Available: <https://www.rfbeam.ch/product?id=18>
- [39] S. M. M. Islam, A. Sylvester, G. Orpilla, and V. M. Lubecke, "Respiratory feature extraction for radar-based continuous identity authentication," in *Proc. IEEE Radio Wireless Symp. (RWS)*, San Antonio, TX, USA, Jan. 2020, pp. 119–122.
- [40] G. Bencherit, "Breathing pattern in humans: Diversity and individuality," *Respirat. Physiol.*, vol. 122, nos. 2–3, pp. 123–129, Sep. 2000, doi: [10.1016/S0034-5687\(00\)00154-7](https://doi.org/10.1016/S0034-5687(00)00154-7).
- [41] S. B. Kotsiantis, "Supervised machine learning: A review of classification techniques," *Inform., Int. J. Comput. Inform.*, vol. 31, pp. 249–268, 2007.
- [42] S. Suthaharan, "Support vector machine," in *Machine Learning Models and Algorithms for Big Data Classification: Thinking With Examples For Effective Learning*, vol. 36. Boston, MA, USA: Springer, 2015, pp. 207–235.
- [43] Accessed: Feb. 1, 2022. [Online]. Available: <https://www.mathworks.com/help/stats/classificationlearner-app.html>



- [44] E. Vanegas, R. Igual, and I. Plaza, "Sensing systems for respiration monitoring: A technical systematic review," *Sensors*, vol. 20, no. 18, p. 5446, Sep. 2020, doi: [10.3390/s20185446](https://doi.org/10.3390/s20185446).
- [45] S. M. M. Islam, A. Rahman, E. Yavari, M. Baboli, O. Boric-Lubecke, and V. M. Lubecke, "Identity authentication of OSA patients using microwave Doppler radar and machine learning classifiers," in *Proc. IEEE Radio Wireless Symp. (RWS)*, San Antonio, TX, USA, Jan. 2020, pp. 251–254, doi: [10.1109/RWS45077.2020.9049983](https://doi.org/10.1109/RWS45077.2020.9049983).
- [46] C. Li and J. Lin, "Random body movement cancellation in Doppler radar vital sign detection," *IEEE Trans. Microw. Theory Techn.*, vol. 56, no. 12, pp. 3143–3152, Dec. 2008, doi: [10.1109/TMTT.2008.2007139](https://doi.org/10.1109/TMTT.2008.2007139).
- [47] C. Gu, G. Wang, T. Inoue, and C. Li, "Doppler radar vital sign detection with random body movement cancellation based on adaptive phase compensation," in *IEEE MTT-S Int. Microw. Symp. Dig.*, Seattle, WA, USA, Jun. 2013, pp. 1–3, doi: [10.1109/MWSYM.2013.6697618](https://doi.org/10.1109/MWSYM.2013.6697618).
- [48] C. Gu, G. Wang, Y. Li, T. Inoue, and C. Li, "A hybrid radar-camera sensing system with phase compensation for random body movement cancellation in Doppler vital sign detection," *IEEE Trans. Microw. Theory Techn.*, vol. 61, no. 12, pp. 4678–4688, Dec. 2013, doi: [10.1109/TMTT.2013.2288226](https://doi.org/10.1109/TMTT.2013.2288226).
- [49] S. M. M. Islam, L. C. Lubecke, C. Grado, and V. M. Lubecke, "An adaptive filter technique for platform motion compensation in unmanned aerial vehicle based remote life sensing radar," in *Proc. 50th Eur. Microw. Conf. (EuMC)*, Utrecht, The Netherlands, Jan. 2021, pp. 10–15.
- [50] W. Massagram, V. M. Lubecke, and O. Boric-Lubecke, "Feasibility assessment of Doppler radar long-term physiological measurements," in *Proc. Annu. Int. Conf. IEEE Eng. Med. Biol. Soc.*, Aug. 2011, pp. 1544–1547, doi: [10.1109/IEMBS.2011.6090450](https://doi.org/10.1109/IEMBS.2011.6090450).
- [51] J. Xiong, H. Hong, H. Zhang, N. Wang, H. Chu, and X. Zhu, "Multi-target respiration detection with adaptive digital beamforming technique based on SIMO radar," *IEEE Trans. Microw. Theory Techn.*, vol. 68, no. 11, pp. 4814–4824, Nov. 2020, doi: [10.1109/TMTT.2020.3020082](https://doi.org/10.1109/TMTT.2020.3020082).
- [52] L. Zhang, Y. Liu, H. Hong, X. Zhu, and C. Li, "Noncontact multi-target respiration sensing using SIMO radar with UBSS method," *IEEE Microw. Wireless Compon. Lett.*, vol. 32, no. 3, pp. 210–213, Mar. 2022, doi: [10.1109/LMWC.2021.3138767](https://doi.org/10.1109/LMWC.2021.3138767).



**Shekh M. M. Islam** (Member, IEEE) received the B.Sc. (Hons.) and M.Sc. degrees in electrical and electronic engineering from the University of Dhaka, Dhaka, Bangladesh, in 2012 and 2014, respectively, and the Ph.D. degree in electrical engineering from the University of Hawaii at Mānoa, Honolulu, HI, USA, in December 2020, with a focus on biomedical applications incorporating RF/microwave technologies.

From 2014 to 2016, he worked as a Lecturer with the Department of Electrical and Electronic

Engineering, University of Dhaka. He is currently working as an Assistant Professor with the Department of Electrical and Electronic Engineering, University of Dhaka. His research interests include radar systems, antenna array signal processing, adaptive filter technique, and machine learning classifiers for pattern recognition. In summer 2019, he also worked as a Radar System and Applications Engineering Intern with ON Semiconductor, Phoenix, AZ, USA.

Dr. Islam has been serving as an Affiliate Member of the Technical Committee for the MTT-28 Biological Effects and Medical Applications of the IEEE Microwave Theory and Technique Society. He was a recipient of the 2020 University of Hawaii at Mānoa Department of Electrical Engineering Research Excellence Award. He was also the Student Paper Finalist at IEEE Radio Wireless Week (RWW 2019) Conference, which was held in FL, USA. He has also been serving as an Editorial Board Member for *Frontiers in Physiology* journal and a Review Editor for IEEE ACCESS, IEEE SENSORS JOURNAL, IEEE TRANSACTIONS ON MICROWAVE THEORY AND TECHNIQUES, *Sensors* (MDPI), *Frontiers in Sensors*, and *Frontiers in Communication and Network*.



**Olga Boric-Lubecke** (Fellow, IEEE) received the B.Sc. degree from the University of Belgrade, Belgrade, Serbia, in 1989, the M.S. degree from the California Institute of Technology, Pasadena, CA, USA, in 1990, and the Ph.D. degree from the University of California at Los Angeles, Los Angeles, CA, USA, in 1995, all in electrical engineering.

She was a Visiting Researcher with the Institute of Physical and Chemical Research (RIKEN), Sendai, Japan, and a Resident Research Associate with the NASA Jet Propulsion Laboratory, Pasadena, CA,

USA. She is currently a Professor of electrical and computer engineering at the University of Hawaii at Mānoa (UH), Honolulu, HI, USA. Prior to joining UH, she was with Bell Laboratories, Lucent Technologies, Murray Hill, NJ, USA, where she conducted research in RFIC technology and biomedical applications of wireless systems. She co-founded and served as a Chief Technical Advisor for a startup company, Kai Medical, Honolulu. She is also a Co-Founder and the President of Adnoviv, Inc., Honolulu. She has authored over 200 journal and conference publications, two books, and several book chapters. She holds two patents and her research has been featured by various media outlets. Her current research interests include wireless circuits and systems, biomedical applications, and renewable energy.

Dr. Boric-Lubecke is a Distinguished Member of the National Academy of Inventors, UH Chapter, and a Foreign Member of the Academy of Engineering of Serbia. She was a co-recipient of the Emerging Technology Award at TechConnect 2007. She was the adviser-author of several award-winning IEEE Microwave Theory and Techniques Society (IEEE MTT-S) and IEEE Engineering in Medicine and Biology Society (EMB-S) student papers. She has served as the Workshop Chair for the 2003 IEEE IMS, the Technical Program Vice-Chair for 2007 IEEE IMS, the Technical Program Co-Chair for 2017 IEEE IMS, and a 2018 IEEE IMS Technical Program Advisor. She has served as an Associate Editor for the IEEE MICROWAVE AND WIRELESS COMPONENTS LETTERS and the IEEE TRANSACTIONS ON MICROWAVE THEORY AND TECHNIQUES and an IEEE MTT Fellow Selection Committee Member.



**Victor M. Lubecke** (Fellow, IEEE) received the M.S. and Ph.D. degrees in electrical engineering from the California Institute of Technology, Pasadena, CA, USA, in 1990 and 1995, respectively.

He is currently a Professor of electrical and computer engineering at the University of Hawaii at Mānoa, Honolulu, HI, USA. He was previously with Bell Laboratories, Lucent Technologies, Murray Hill, NJ, USA, where his research focused on remote sensing technologies for biomedical and

industrial applications, and on microelectromechanical systems (MEMS) and 3-D wafer-scale integration technologies for wireless and optical communications. Before that, he was with the NASA Jet Propulsion Laboratory (JPL), Pasadena, and the Institute for Physical and Chemical Research (RIKEN), Japan, where his research involved terahertz and MEMS receiver technologies for space remote sensing and communications applications. He has published over 200 peer-reviewed research articles, holds eight U.S. patents, and co-founded two high-tech startup companies. His current research interests include remote sensing, biomedical sensors, MEMS, heterogeneous integration, and microwave/terahertz radio.

Dr. Lubecke is an emeritus Distinguished Microwave Lecturer of the IEEE Microwave Theory and Techniques (MTT) Society and a Speakers Bureau Speaker. He has served as a Topic Editor for the IEEE TRANSACTIONS ON TERAHERTZ SCIENCE AND TECHNOLOGY, the Vice-Chair for the 2017 IEEE International Microwave Symposium (IMS), and a member of the MTT Technical Committees for Terahertz Technology and Applications and Biological Effects and Medical Applications.